Clean Technologies and Environmental Policy (2018) 20:1663–1684
https://doi.org/10.1007/s10098-018-1486-6

ORIGINAL PAPER

Energy, exergy and techno-economic analysis for biobutanol production: a multi-objective optimization approach based on economic and environmental criteria

Juan José Quiroz-Ramírez[1,2] · **Eduardo Sánchez-Ramírez**[1] · **Juan Gabriel Segovia-Hernández**[1]

Received: 8 May 2017 / Accepted: 4 January 2018 / Published online: 25 January 2018

Abstract

Currently, butanol obtained by fermentation is considered as potential biofuel. In this work, it has been simulated and optimized a process to produce acetone, butanol and ethanol by means of lignocellulosic material. To accomplish this task, initially, it was planned the raw material selection, followed by the simulation in MATLAB of simultaneous saccharification, fermentation and separation reactor (SFS) and finally, the stream coming from fermentation was purified. The separation stage was selected from three different options to purify that effluent. The entire process was evaluated under a robust optimization process considering environmental, economic and energetic objective functions by means of a hybrid stochastic method, differential evolution with tabu list. The obtained results showed that the best scheme to produce and purify butanol was the SFS-3C, which considers thermally coupled columns to purify acetone, butanol and ethanol. In general terms, it was obtained as result 0.138 $\$/\text{kg}_{\text{butanol}}$, 0.132 $\text{points}/\text{kg}_{\text{butanol}}$ and 66.8 regarding to the total annual cost, environmental impact and exergy efficiency, respectively.

Keywords Biobutanol · Multi-objective optimization · Energy · Exergy · Techno-economic analysis

List of symbols

ABE	Acetone–butanol–ethanol
C_{TM}	Capital cost of the plant
C_{ut}	Utility costs
DDE	Dynamic data exchange
DE	Differential evolution
DETL	Differential evolution with tabu list
D_{cn}	Column diameter
F_{ext}	Extractant flow
F_{rn}	Distillate fluxes
TAC	Total annual cost
LLE	Liquid–liquid extraction
LCA	Life cycle assessment
N_{tn}	Total column stages
N_{fn}	Feed stages
ROI	Return of investment
SFS	Integrated reactor saccharification–fermentation with simultaneous recovery
R_{rn}	Reflux ratio
TAC	Total annual cost
TL	Tabu list
x_m	Vectors of required purities
y_m	Vectors of obtained purities
F	Mass flow
V	Volume
S	Substrate
x	Molar fraction
C	Amount of mass in the reactor
GEI99	Global ecoindicator 99
NEB	Net energy balance
η	Exergy efficiency
NPV	Net present value
IES	Ideal energy efficiency of separation
A	Raw material
X	Amount of biomass used
D	Dilution rate
ENZ	Amount of enzyme
N_{fni}	Feed stage
F_{rni}	Flow of interconnection

✉ Juan José Quiroz-Ramírez
jjqr111@hotmail.com

[1] Chemical Engineering Department, Universidad de Guanajuato, Noria Alta s/n, 36050 Guanajuato, Gto, Mexico

[2] CONACyT – CIATEC A.C. Centro de Innovación Aplicada en Tecnologías Competitivas, Omega 201, Col. Industrial Delta, 37545 León, Gto, Mexico

MODE-TL	Multi-objetive differential evolution with tabu list
R_s	Yield for butanol fermentation
LHV	Lower heating value of butanol
H_s	Energy consumption for purification
PU_b	Quantity of each raw material
RMU_b	Unitary ecoindicator of raw material
EI99PUR	Ecoindicator of purification stage
β_b	Amount of chemical released per unit of reference flow
$\alpha_{b,k}$	Damage caused in category
ω_{d}	Weighting factor for damage in category
δ_{d}	Normalization factor for damage
EI99RM	Ecoindicator 99 of total raw material used
C_{GR}	Total grassroots costs
$C_{\mathrm{BM},i}$	Module cost of the equipment
$C_{\mathrm{BM},i}$	Module cost of the equipment considers real operation
C_{R}	Reactor cost
C_{T}	Column cost
C_{IN}	Condenser cost
C_{IE}	Initial investment
C_{E}	Electricity cost
C_{V}	Steam cost
C_{AE}	Cooling water cost
C_{S}	Substrate cost
C_{ENZ}	Enzyme cost
C_{Ex}	Cost due to extractant lost
NEB	Net energy balance
LHV	Lower heating value
IES	Ideal energy efficiency of separation
R_s	Yield ABE
H_s	Energy consumption for purification
NE_t	Net earnings value
FTDC_t	Depreciable capital investment
φ	Net earnings after tax rate
Rev_t	Revenues
FOC_t	Facility operating
TOC_t	Transportation
$E_{x,\mathrm{ABE}}$	Exergy of produced ABE (MW)
$E_{x,\mathrm{biomass}}$	Exergy of biomass (MW)
$E_{x,\mathrm{heating}}$	Exergy of heating (MW)
$E_{x,\mathrm{reactor}}$	Exergy of reactor (MW)

Introduction

In recent years, both social and political pressures trying to diminish the use of fossil fuels have acquired a major exigency. In the past years, butanol has attracted a constant interest because of its thermodynamic properties, some of them quite similar to gasoline. Those butanol properties, such as high energy density, low volatility, less hygroscopic, etc., have pointed out butanol as an interesting biofuel (Xue et al. 2013).

Biobutanol is produced via the fermentation by means of a *Clostridium* bacteria obtaining as main products acetone, butanol and ethanol (ABE) in a typical relation of 3:6:1 (Cooksley et al. 2012; Niemistö et al. 2014). Despite biobutanol properties, this process should overcome several challenges related with butanol concentration and volumetric productivities, as well as diminishment in by-products (Xue et al. 2013). In this manner, the performance of this process is limited by the high substrate cost and both inhibition by substrate and butanol concentration (near to 20 g/L). These hurdles produce diluted effluents, and consequently the energy requirements in downstream process increase as well (Kiss et al. 2016). Having an aim to reduce substrate cost, it is proposed lignocellulosic biomass as fermentable substrate because of its low economic and environmental impact. Currently, a wide variety of substrates have been proposed; the options vary from saccharose (Parekh and Blaschek 1999; Tashiro and Sonomoto 2010), domestic and agricultural wastes (Jang et al. 2012; Niemistö et al. 2014), biomass from algae (Ranjan and Moholkar 2009; Jang et al. 2012), wheat straw, starch (Ranjan and Moholkar 2009), whey (Ranjan and Moholkar 2009) among others. However, to select any raw material it is necessary to consider the nature of the raw material and its availability, and this task must be done to find a feasible combination to produce sustainable butanol.

Because of the high content of lignocellulose, it is necessary to perform a pretreatment stage. In this stage, the hemicellulose is converted to xylose and a further diminishment in crystalline cellulose is observed. Several options are currently available, for example, diluted acid, steam explosion or enzymatic hydrolysis. Currently, enzymatic hydrolysis is the most accurate option according to several authors (Andrié et al. 2010; Qureshi et al. 2014). Because of diluted products, it is estimated that the necessary energy to increase the butanol concentration from 0.5 to 99.9% wt in a binary system butanol–water is near 79.5 MJ/kg, much more energy than that contained in butanol. Under this scenario, it has been proposed integrated systems (saccharification–fermentation) where the products can be withdrawn avoiding inhibition by butanol concentration (Qureshi et al. 2005; Mariano et al. 2012) increasing also the concentration of products after fermentation. On the other hand, some reports have proved that the hybrid process, which involves a liquid–liquid extractive column, can reduce the energy requirements since it can separate in a single column the azeotropes involved in the mixture coming from fermenter. So, much energy used to concentrate the ABE compounds is saved in a single stage (Errico et al. 2016).

Because of the above-mention fact, much attention has been focused on the process in such manner that energy requirements do not exceed the contained energy of butanol. The main purification process and their average energy requirements are summarized in Table 1. In this manner, an effective alternative to make more profitable the biobutanol production uses an integrated reactor followed by a hybrid process to purify the effluent coming from fermenter.

Since the energy demand is a primary measure to evaluate a process, the evaluation of exergy seems a reliable option to evaluate and improve energy systems. Also, it can help to understand the benefits of use a green alternative in comparison with the traditional energetic point of view. For example, different works show how to use the exergy efficiency as comparison among several schemes (Rosen et al. 2008, Gassner and Marechal 2013; Bechara et al. 2016). With this in mind, this research describes a quantitative analysis of efficiency based on an exergy analysis as additional criteria to select the best process to produce and purify butanol. This analysis also considers economic and environmental criteria to complement this selection.

Therefore, the aims of this research were: (1) to evaluate the biobutanol production considering several raw materials, all lignocellulosic materials evaluated through an environmental and economic indicators, such as the ecoindicator 99, the total annual cost (TAC) and the net present value (NPV) and (2) to perform an analysis of the better schemes to produce biobutanol having as base both exergy and energy requirements.

Methodology

Problem statement

The complete problem to be solved can be described as follows: from a series of raw materials, it must be planned the correct selection of them considering the amount of sugar on each raw material, its availability through the year and the economic and environmental impact. Those raw materials will be fed to an integrated reactor to simultaneously carry on the saccharification and fermentation process. As a product, a stream will be produced with different characteristics according to the selected raw materials (see Fig. 1). In this manner, because of the complexity of the process, it is necessary to perform a rigorous optimization to handle this kind of nonlinearity and potential non-convexity. The next section will briefly describe each analyzed section.

Biomass

The raw material for fermentation is the main parameter to warranty economic profitability of any fermentation process (Lenz and Morelra 1980; Gapes 2000; Qureshi and Blaschek 2000, 2001). The substrate in fermentation represents near 60% of the production cost (Qureshi and Blaschek 2000). Commonly chemical components produced by fermentation are preferably produced in small plants to satisfy the specific needs of communities. Besides, the cost of the substrate must be optimized to establish how much the maximum is to be paid to generate profit and return of investment (Gapes 2000).

Table 1 Comparison of several integrated butanol recovery processes (Groot et al. 1992; Oudshoorn et al. 2009; Xue et al. 2014)

Process	Advantage	Disadvantages	Selectivity	Energy requirements (MJ/kg)
Pervaporation	High selectivity	Cost of the membrane	2–209	2–145
Liquid–liquid extraction	High selectivity	Formation of emulsion Cost of extractant Toxic to the culture Recovery and loss of the extractant	1.2–4100	7.7 (26 for ABE)
Gas stripping	It does not soil or damage the crop Easy to operate	Low selectivity Low efficiency	4–22	14–31
Vacuum fermentation	It does not soil or damage the crop Easy to operate	Low selectivity Low efficiency	15.5–33.8	–
Perstraction	High selectivity Low toxicity to the crop	Formation of emulsion Cost of material	1.2–4100	7–7
Adsorption	Easy to operate Under energy requirement	High cost of the material Low selectivity Adsorption regeneration	130–630	1.333

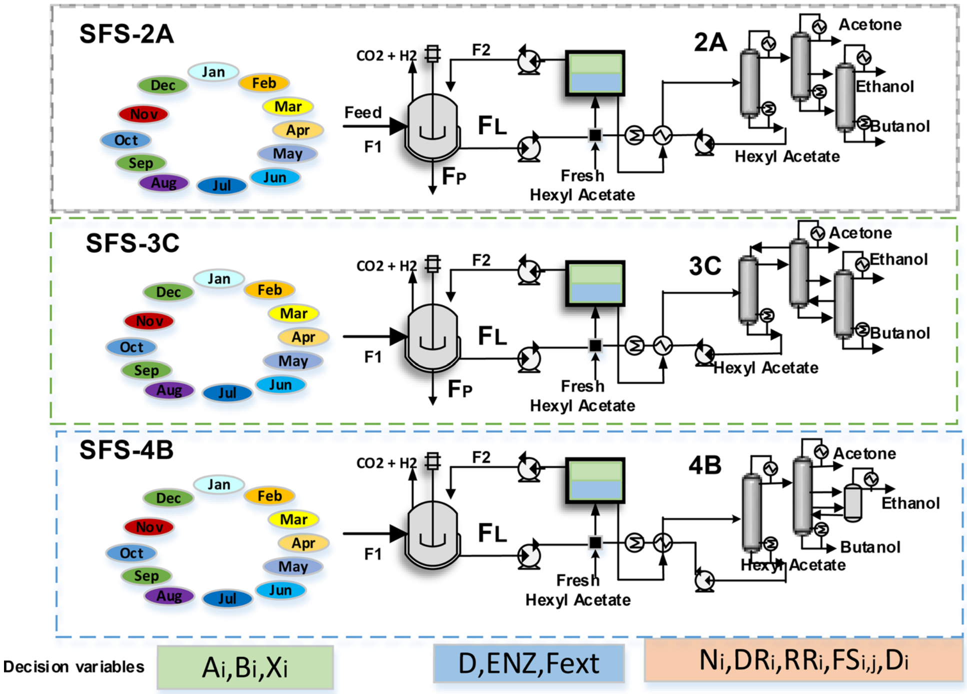

Fig. 1 Schematic representation of the butanol production process including the raw material selection, saccharification–fermentation and downstream process

From all available raw materials, the lignocellulosic material is considered the most promising because of its availability, sugar content and its renewable nature so far. In this research, as boundaries in raw material selection, we consider the available raw material in México which is presented in Table 2.

Integrated reactor saccharification–fermentation with simultaneous recovery (SFS)

An advantage of new technologies is to improve the productivity in a reactor by means of integration of fermentation and recovery stages (Maddox 1989). Simulation of simultaneous fermentation and saccharification separation was performed in MATLAB®.

To describe the behavior of enzymatic hydrolysis in the biomass, it has been considered the kinetic model developed by Kadam et al. (2004). This model includes a reaction for: (2) decomposition of cellulose to cellobiose and glucose; (2) hydrolysis of cellobiose to glucose; (3) enzymatic adsorption; (4) substrate reactivity; and (5) effect of temperature on hydrolysis.

The parameter which describes the enzymatic reactivity was adapted considering a continuous process with changes in cellulose concentration by means of Eq. 1 (Díaz and Tost 2016a, b).

$$R_S = \frac{S(t)\cdot V(t) + \int_0^{t_f} x_{BS}\cdot F_B \cdot \mathrm{d}t}{x_{1s}\cdot F_1 \cdot \left(t_f - t_a\right) + S(0)\cdot V(0)} \quad (1)$$

Table 2 Ecoindicator 99 for processed feedstock amount for biofuel production (Santibañez-Aguilar et al. 2014)

	Raw material	Cellulose %(w/w)	Hemicellulose %(w/w)	Lignin %(w/w)	Cost (USD/ton)	Ecoindicator 99 (points/ton)
1	Wood chips	40	24	18	27	39.31
2	Wheat straw	30	50	15	38.29	11.84
3	Sugar cane	43	24	20	30.49	1.84
4	Wheat	30	39	18	50.68	13.1
5	Corn grain	41	23	12	55.86	17.16
6	Sorghum grain	20	42	18	53.2	5.85
7	Cassava root	30	22	22	88.2	42.05
8	Sugar beet	35	29	22	27.5	2.75
9	Sweet sorghum	22	48	18	16.1	5.85

where F_1 represents the feed flow, F_B are the flow of bleeding; S is the concentration of cellulose into the reactor (mmol/L); V is the volume (L); x_{BS} is the mole fraction of cellulose into the reactor; x_{1_s} is the mole fraction of cellulose in the feed stream; t_a is the initial time of continuous feed; and t_f is the end time of fermentation.

On the other hand, the kinetic model to describe the production of ABE from lignocellulosic sugars is based on the model proposed by Shinto et al. (2007, 2008), which considers the participation of *clostridium acetobutilum* bacteria to ferment glucose and xylose simultaneously. This model considers several fermentation stages: cellular growth, substrate consumption and biobutanol production. In this manner, the global balance in the integrated reactor is described as follows:

$$\frac{dCi}{dt} = R_i \cdot V_F + F_1 \cdot x_{1i} - F_p \cdot x_{Pi} + F_L \cdot x_{Li} \tag{2}$$

where C_i is the concentration of each component: butanol, ethanol, acetone, butyric acid, acetic acid, glucose and xylose, and all F's are flow streams considered as input or outputs in the integrated reactor (see Fig. 1). F_1 is the flow of feedstock, F_p is the flow purge and F_L is the flow of bleeding, x is the molar fraction. R_i (mmol/h/L) is the reaction rates of the fermentation and the hydrolysis. V_F is the volume of liquid fraction plus the solid fraction.

As a separation stage on the integrated reactor, the liquid–liquid extraction was selected, having as extractant agent *N*-hexyl-acetate according to the work of Barton and Daugulis (1992) and Groot et al. (1990). This selection was carried out considering the high partition coefficient, high selectivity, low cost and medium boiling point.

To guarantee a more competitive fermentation process, the best condition to achieve must be identified to achieve good values concerning some bioindicators (productivity, yield, product concentration), all of them evaluated under the correct selection of raw material used as feed in the fermenter. Those best conditions are probably only provided if the model is optimized searching for the best values of the objective functions, varying the amount of enzyme added, the dilution rate and the amount of extractant agent. For example, as a result some direct relationship might be observed, if high amount of extractant is added, it is easier to separate the compounds. However, the amount of extractant agent increases the energy required in further separation. It is considered that the reactor is at a steady state without variations in the outlet stream (Quiroz-Ramírez et al. 2017); at this moment the effluent is fed to the downstream process. Note the time to reach the steady state has not been taken into consideration.

Separation and purification stage

To perform the purification of biobutanol after fermentation, three different schemes were considered. The first one is a conventional system with a side stream, the second one is a thermally coupled design and finally, the third one is a thermodynamic equivalent design (see Fig. 1). Those designs were previously presented by Errico et al. (2016) as the most promising designs among several options to separate an effluent coming from fermenter. In this work, those separation schemes were modeled in Aspen Plus, using the RADFRAC module, which considers the entire set of MESH equations. Note that these process models were robust and thermodynamically rigorous. The NRTL model was used to calculate the activity coefficient for the liquid phase and the Hayden–O'Connell equation for the vapor phase (Wooley and Putsche 1996; Oudshoorn et al. 2009a; van der Merwe et al. 2013).

Besides, both processes were modeled in MATLAB and Aspen Plus, linked with each other. In this manner, the feed stream (previously proposed by the planning) was sent as a vector to MATLAB where the saccharification–fermentation and recovery are modeled. As the reactor products mainly obtained were acetone, butanol, ethanol and *N*-hexyl-acetate, it was also possible to calculate all bioindicators, productivity, yields and product concentration. This produced flow was further used as a feed stream in the purification process. Finally, Aspen Plus generates the necessary energy and mass balances to calculate all objective functions.

The raw material planning, the integrated reactor saccharification–fermentation with simultaneous recovery (SFS) and the separation unit are integrated in a single process.

Those integrated processes are referred to as SFS-3C, SFS-2A and SFS-4B according to the purification stage they are formed (see Fig. 1).

Multi-objective optimization

The process design to produce butanol is an example of a highly nonlinear and potentially non-convex system because of all of the equations included in the process model. All those equations are included in the objective function, and the minimization of those objective functions is subject to recoveries and purity products on each flow stream. The problem is set as:

$$
\begin{aligned}
&\mathrm{Min}(\mathrm{TAC}, \mathrm{GEI99}, \mathrm{NEB}, -\eta, -\mathrm{NPV}, -\mathrm{IES}) \\
&\quad = f\left(A_i, X_i, D, \mathrm{ENZ}, F_{\mathrm{ext}}, N_{tni}, N_{fni}, R_{rni}, F_{rni}, D_{cni}\right) \\
&\text{Subject to} \quad \vec{y}_m \geq \vec{x}_m
\end{aligned} \tag{3}
$$

where A_i is the raw material, X_i is the amount of biomass used during all year long, D is the dilution rate in fermenter, ENZ is the amount of enzyme in fermenter, N_{tn} is the total theoretical stages in the columns, R_{rn} the reflux ratio, F_m the distillate flow, D_{cn} the column diameter, y_m and x_m are purity and recovery vector for the m components, respectively. Table 3 summarizes a brief description and the range on each variable.

In this research, we have used a hybrid stochastic multi-objective algorithm, differential evolution with tabu list (DETL) previously presented by Sharma and Rangaiah (2010, 2013). The DETL algorithm specifically includes the evaluation stages of differential evolution, and furthermore, the tabu list concept (TL) can be used to avoid the revisit of search space by keeping a record of recently visited points. This can avoid unnecessary function evaluations, and because of this the computational efficiency is improved and the diversity is also increased (Srinivas and Rangaiah 2007; Sharma and Rangaiah 2010, 2013). The implementation of the multi-objective optimization approach was performed using a hybrid platform using a Microsoft Excel program of MODE-TL coupled with MATLAB and Aspen Plus (see Fig. 2).

For the multi-objective optimization, we have used the following parameters for MODE-TL method: 200 individuals, 500 generations, a tabu list of 50% of total individuals, a tabu radius of 2.5E^{-06}, 0.80 and 0.6 for crossover and mutation fractions, respectively. The best parameter values are obtained by a preliminar tuning process of values based on both previous work and computational efficiency of the algorithm (Sharma and Rangaiah 2013).

Actually, much research has used this algorithm to handle several problems in chemical engineering in example those presented by Miranda-Galindo et al. (2014), Vázquez-Castillo et al. (2015), Errico et al. (2016), and other applications in the form of global optimization (Yerramsetty and Murty 2008; Kheawhom 2010; Bonilla-Petriciolet et al. 2010; Kumar et al. 2011; Vakili et al. 2011; Bhattacharya et al. 2011, among others). In all these studies, the use of this algorithm has proved to be robust enough to solve highly nonlinear problems.

Table 3 Definition of optimization problem: decision variables and measured parameters

Block	Decision variables	Optimization range
Raw material	Type of raw material (9 variables) (–)	[0;1]
Hydrolysis	Enzymes ratio (2 variables) (kg/kg)	[0;1]
Reactor	Dilution rate (h^{-1})	[0.01–0.3]
Decanter	Solvent to feed ratio (kg/kg)	[30–60]
Distillation	Number of theoretical stages (3 variables) (–)	[15–80]
	Reflux ratio (3 variables) (–)	[0.1–60]
	Feed stage (5 variables) (–)	[3–79]
	Interlinking stages (8 variables) (–)	[3–79]
	Side stream stage (5 variables) (–)	[3–79]
	Column diameter (4 variables) (m)	[2–4.5]
	Distillate flow rate (9 variables) (kg h^{-1})	[$2x - 4.5x$]
	Side stream flow rate (9 videos) (kg h^{-1})	[$2x - 4.5x$]

x represents the flow of the sum of the components coming out of the corresponding current

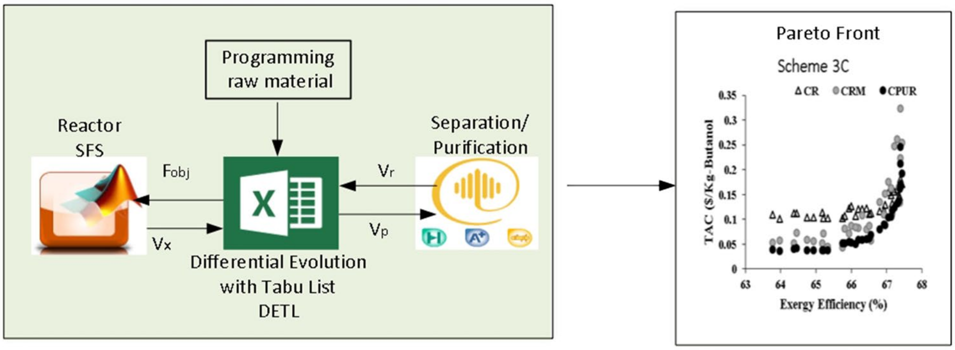

Fig. 2 Optimization strategy considering the connection among MATLAB, AspenTech and MS Excel

Environmental objective function

The introduction of environmental issues as an objective function has been satisfactorily assessed in different works and methodologies (Azapagic and Clift 1999; Gebreslassie et al. 2009; López-Maldonado et al. 2011; Vázquez-Castillo et al. 2015). The life cycle analysis is an environmental tool to asses in a quantitative way the environmental loads of a process. This approach includes raw material extractions, manufacturing, distribution, recycled and waste disposition.

The ecoindicator 99 is a methodology based on life cycle analysis (see Fig. 3). This environmental index is able to give a score to any process or product to calculate its environmental load. In the ecoindicator 99 methodology, 11 impact categories are considered (Goedkoop and Spriensma 2000):

1. Carcinogenic effects on humans
2. Respiratory effects on humans that are caused by organic substances
3. Respiratory effects on humans caused by inorganic substances
4. Damage to human health that is caused by climate change
5. Human health effects that are caused by ionizing radiations
6. Human health effects that are caused by ozone layer depletion
7. Damage to ecosystem quality that is caused by ecosystem toxic emissions
8. Damage to ecosystem quality that is caused by the combined effect of acidification and eutrophication
9. Damage to ecosystem quality that is caused by land occupation and land conversion
10. Damage to resources caused by the extraction of minerals
11. Damage to resources caused by extraction of fossil fuels.

These 11 categories are divided into three major damages categories: (1) human health, (2) ecosystem quality and (3) resources depletion.

Since in this study the selection of raw material is a main issue, the environmental load generated by the biomass should be carefully calculated. Due to this, during the fermentation, the environmental impact can be estimated according to Eq. 4, RMU_b is the unitary ecoindicator of each raw material and PU_b is the quantity of each raw material used, and the environmental impact caused by the purification stage (EI99PUR) is represented in Eq. 5. β_b represents the total amount of chemical released per unit of reference flow due to direct emissions, $\alpha_{b,k}$ is the damage caused in category k per unit of chemical b released to the environment, ω_{d} is a weighting factor for damage in category d, and δ_{d} is the normalization factor for damage (Goedkoop and Spriensma 2000), as seen in the following

$$\mathrm{EI99RM}_b = \frac{\mathrm{EI99RMU}_b \sum_{g} \sum_{t} PU_b}{F_{\mathrm{butanol}}} \quad \forall t \tag{4}$$

$$\mathrm{EI99PUR}_b = \frac{\sum_{b} \sum_{d} \sum_{k \in K} \delta_d \omega_d \beta_b \alpha_{b,k}}{F_{\mathrm{butanol}}} \quad \forall b \tag{5}$$

So the overall environmental damage per category (GEI99) is estimated as follows:

$$\mathrm{GEI99} = \mathrm{EI99RM}_b + \mathrm{EI99PUR}_b \quad \forall b \tag{6}$$

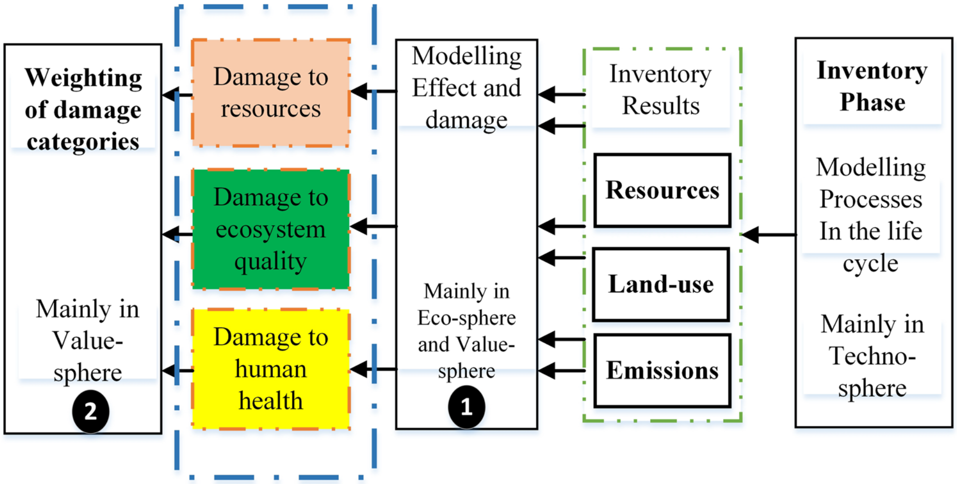

Fig. 3 Environmental impact assessment in the methodology of the ecoindicator 99 (EI99) (adapted from Goedkoop and Spriensma 2000)

Economic analysis

In the methodology of this work, the thermodynamic conditions have been considered as decision variables. Once those conditions are determined in the model, the performance and cost are calculated. This methodology differs from the conventional thermo-economic approaches where the equipment size is considered as variable decision and the total investment cost is estimated with the nominal capacity of the component (Tijmensen et al. 2002).

The estimate of investment presented in this work is obtained performing a simplified sizing of the main equipment. This methodology takes into account that the equipment cost mainly depends on the size and building materials, and it is also influenced by the process condition, such as temperature, pressure and auxiliary services. Thus, the available information allows to connect the investment cost of the process with its thermodynamic and operative conditions. Following the method presented by Turton et al. (2012), the total grassroots costs (C_{GR}) can be related with the equipment purchase cost according to the next equation:

$$C_{\mathrm{GR}} = \left(1 + c_1\right) \sum_i C_{\mathrm{BM},i} + c_2 \sum C^0_{\mathrm{BM},i} \tag{7}$$

where $C_{\mathrm{BM},i}$ is the module cost of the equipment i on standard condition (atmospheric pressure and carbon steel as building material), $C_{\mathrm{BM},i}$ considers real operation conditions, and c_1 and c_2 represents additional spends related with the building of the plant. Table 4 summarizes the main parameters used in this economic evaluation.

Equipment cost

To calculate the total annual cost (TAC) used as objective function, we used the method published by Guthrie (1969), which was modified by Ulrich (1984). It performs cost estimation of an industrial plant separated in units using equations published by Turton et al. (2012). So, this economic index is calculated as follows:

$$\mathrm{TAC}\left(\mathrm{US\$/\,kg - ABE}\right) = \frac{\frac{\sum_{i=1}^{n} C_{TM,i}}{n} + \frac{\sum_{j=1}^{n} C_{ut,j}}{t_{ri}}}{F_{\mathrm{butanol}} \cdot t_o} \tag{8}$$

where TAC is the total annual cost, $C_{\mathrm{TM,i}}$ is the capital cost of the plant, n is the total number of individual units and $C_{\mathrm{ut},j}$ is the cost of services, F_{butanol} is the production flow ($\mathrm{kg}_{\mathrm{butanol}}$/h), and t_{ri}, is the payback period (3 years). It was assumed that the plant is running 8500 h per year (t_{o}), respectively.

The total investment is given by:

$$\text{Total investment} = C_{\mathrm{R}} + C_{\mathrm{T}} + C_{\mathrm{IN}} + C_{\mathrm{IE}} \tag{9}$$

where C_{R}, C_{T}, C_{IN} and C_{IE} correspond to the reactor cost, column cost, condenser cost and initial investment, respectively. All costs were calculated as functions of the installation cost.

The annualized operative cost is calculated as follows:

$$\text{Operating cost} = C_{\mathrm{E}} + C_{\mathrm{V}} + C_{\mathrm{AE}} + C_{\mathrm{S}} + C_{\mathrm{ENZ}} + C_{\mathrm{Ex}} \tag{10}$$

where C_{E}, C_{V}, C_{AE}, C_{S}, C_{ENZ} and C_{Ex} represent the electricity cost, steam cost, cooling water cost, substrate cost, enzyme cost and cost due to extractant lost, respectively.

The payback period was considered as 3 years (Luyben and Chien 2011), and it is assumed the plant runs 8500 h/year. Also, the following costs for heating and cooling were taken into account: high-pressure steam (42 bar, 254 °C, \$9.88/GJ), medium-pressure steam (11 bar, 184 °C, \$8.22/GJ), low-pressure steam (6 bar, 160 °C, \$7.78/GJ) and cooling water (\$0.72\$/GJ) (Luyben and Chien 2011).

The cost of feedstock was calculated as the sum of all feedstock purchased from each supplier i (F_i):

$$\text{FeedstockCost} = \sum\nolimits_i C_i^{\mathrm{Biomass1}} F_1 + \sum\nolimits_k C_k^{\mathrm{Biomass2}} F_2 \tag{11}$$

where C_i is the raw material cost, F_1 and F_2 is the biomass flux considered as feed stream to the reactor.

However, for further analysis in the production process, the TAC is divided in three areas: the cost associated with raw material (CRM), the cost associated with the reactor

Table 4 Used parameters for the economic evaluation

Parameter	Value	Parameter	Value
Tax rate	34%	Depreciation strategy	10 years linear
Discount rate	10%	Overhead costs	5% CFixed
Working capital cost	5% (CFixed)	Operator salary	USD 3 M/y
Maintenance costs	5% Fixed capital cost (CFixed)	Marshall and Swift index (2006)	1302
Interest rate	6%	Discount period	15 years
Dollar exchange rate	1.5 US\$/e	Butanol price	198\$/ton
Acetone price	119 \$/ton	Ethanol price	158\$/ton

(CR) and the cost of purification (CPUR). Thus, it can be analyzed the behavior of these zones and their effect on the tested objective functions.

Energy balance

The total energy consumption is a key factor when the operative cost is calculated. For such reason, during selection of technology, the energy consumption should be considered as a key parameter for the correct selection of separation technology.

On the other hand, the net energy balance (NEB) is a significant index to evaluate the energy performance in biobutanol production, in other words to evaluate if biobutanol production produces gain or loss of energy.

The net energy balance was addressed as follows: the energy requirements (MJ/h) were divided by the biobutanol mass flow (kg/h) to obtain the specific energy requirement to produce butanol ($\mathrm{MJ/kg_{butanol}}$). This value must be also minimized as small as possible in comparison with the invested energy to produce and separate butanol.

For pure butanol, the energy density is named as LHV (Akinci et al. 2008). According to some authors, the LHV of butanol is approximately 31.5 MJ/kg (Wu et al. 2008). The LHV provides the energy content in 1 kg. of fuel. For ABE fermentation, the energy content also can be considered as, ethanol and acetone, by-products. Thus, to calculate the net energy return is only necessary to subtract the energy content in 1 kg of butanol (LHV) from the energy to produce 1 kg of butanol.

Because of nature of the problem, several butanol flows are handled, so it is necessary a comparative measure for each design. For such purpose, the ideal energy efficiency of separation is used for each system (IES), and this index is calculated through the next equation (Díaz and Tost 2016a, b):

$$\mathrm{IES} = R_s \cdot \left(\mathrm{LHV} - H_s\right) \tag{12}$$

where LHV is considered as the lower heating value of butanol ($\mathrm{MJ_{fuel}/kg_{solvent}}$), H_s is the energy consumption for purification ($\mathrm{MJ_{fuel}/kg_{solvent}}$). The energy efficiency was considered as ideal since only the energetic requirements for purification were taken into account. The performance R_s is the amount of ABE (g) multiplied by the mass of substrate fed (g).

Exergy analysis

The exergy as thermodynamic concept is a measure of the amount of the maximum mechanic work which can be obtained from a stream if it is displaced to the equilibrium with its environment at $T_0 = 25$ °C and $P_0 = 1$ atm.

Besides, exergy is a thermodynamic measure which may be used to evaluate and improve any energetic system. Increasing the energy efficiency is consequently possible to reduce the environmental impact. It has been suggested that the most appropriate relation between the second thermodynamic law and the environmental impact is exergy because it is a measure of the outputs system to the environment (Szargut 1980; Edgerton 1992).

The exergy balance identifies and quantifies the main sources of thermodynamic irreversibility on each process. However, unlike entropy balances, which is only function of the process itself, the exergy balance is a function of both the system and a reference state. Therefore, the choice of this reference point is important for having an idea concerning the availability at each stage of the process. It is particularly significant to evaluate the residual flows released and further mixed with the environment.

With the purification and separation schemes, the thermodynamic efficiency might be calculated using the thermodynamic laws. For such task, it has been used the equation previously proposed by Seader et al. (2011).

Minimum separation work is represented as:

$$W_{\min} = \sum_{\substack{\text{sal del} \\ \text{sistema}}} nb - \sum_{\substack{\text{ent al} \\ \text{sistema}}} nb \tag{13}$$

$$\text{Exergy efficiency}(\eta) = \frac{E_{x,ABE}}{E_{x,\mathrm{biomass}} + E_{x,heating} + E_{x,\mathrm{reactor}}} \tag{14}$$

where $b = h - T_0 s$ is function of exergy, $\mathrm{LW} = T_0 \Delta S_{irr}$ is the waste of work in the system and η the exergy efficiency. To calculate entropy and enthalpy of any stream in the process, Aspen Plus simulator was employed.

Cash flow analysis

All proposed scenarios have been economically evaluated and compared using general sustainable criteria (Turton et al. 2012). The most meaning criteria for economic purposes is the net present value (NPV). If the NPV value is lower than zero, the project is not sustainable. On the other hand, if NPV is higher than zero, the process is profitable. The NPV quantifies the economic performance and is calculated along the discounted annual cash flow for an undefined time. Besides, it represents the sum of present values or effective cash flow discounted along the project life. As results, NPV is a useful tool to determine the net profitability of a project. To calculate the NPV could be used the next equation (Turton et al. 2012).

$$\mathrm{NPV} = \sum_{i=1}^{\mathrm{LT}} \mathrm{DCF}_i = \sum_{i=1}^{\mathrm{LT}} \frac{CF_i}{\left(1 + r_{dc}\right)^i} (\$) \tag{15}$$

The cash flow is calculated as the difference between net earnings NE_t and the fraction of the total depreciable capital investment (FTDC_t):

$$\mathrm{CF}_t = \mathrm{NE}_t - \mathrm{FTDC}_t \quad t = 1, \dots, t-1 \tag{16}$$

Net earnings after tax rate (φ) are determined by the difference between revenues (Rev_t) and expenses related to facility operating (FOC_t) and transportation (TOC_t) costs:

$$\mathrm{NE}_t = (1-\varphi)\left(\mathrm{Rev}_t - \mathrm{FOC}_t - \mathrm{TOC}_t\right) + \varphi \mathrm{DEP}_t \quad \forall t \tag{17}$$

Accordingly, revenues are estimated from the sales of the final products, which involve the delivered flow and the corresponding price (PR_{igt}):

$$\mathrm{Re}v_t = \sum_{i \in SEP(i)} \sum_{g} DTS_{igt} PR_{igt} \quad \forall t \tag{18}$$

Operating costs are given by the product between the production rate and the average inventory levels with the corresponding unit production cost (UPC_{ipgt}) and unit storage cost (USC_{isgt}), respectively:

$$\mathrm{FOC}_t = \sum_{i} \sum_{g} \sum_{p \in IM(i,p)} \mathrm{UPC}_{ipgt} + \mathrm{DC}_t \quad \forall t \tag{19}$$

Disposal cost (DC_t) as part of the operating costs is a term related to the landfill tax (LT_{igt}) to be handled as a consequence of the amount of waste generated in the process (W_{igt}):

$$\mathrm{DC}_t = \sum_{i} \sum_{g} W_{igt} LT_{igt} \quad \forall t \tag{20}$$

Other economic criteria calculated in this work are the return of investment (ROI). This measure is aimed at reducing the complex process of cash flow that takes place in different periods in the future to one single number. The ROI is defined in Eq. (21).

$$\mathrm{ROI}\,(\%) = \frac{\text{Annual net profit}}{\text{Capital cost}} \times 100\% \tag{21}$$

Results and discussion

According to all that was mentioned above, an efficient process design helps to diminish the total energy required in a process. Figure 4 shows the Pareto front generated after the optimization process, and this Pareto front shows the total annual cost evaluated jointly the exergy efficiency. At first sight, it is possible to observe process with relative high exergy efficiency, but those processes also show a high cost (point I). On the other hand, there are several process with low TAC values but with also low exergy efficiency (point III). So, to find a feasible process design it is necessary to select a point inside the Pareto front which does not compromise any objective function. In Fig. 4, this selection is highlighted with a red point (point II). Please note in further figures, this behavior is also observed for the environmental impact, namely a rise in exergy values is observed when the environmental impact rise as well and vice versa.

Figure 4a shows the TAC values evaluated jointly with the exergy efficiency. Note the maximum efficiencies were obtained for the whole process which carries out the purification with the scheme SFS-3C, followed by the schemes SFS-2A and SFS-4B. This thermodynamic equivalent design has exhibited the worse efficiency values. In this manner, the exergy efficiency for such selected points was 66.8, 50.97 and 44.13% for the schemes SFS-3C, SFS-2A and SFS-4B, respectively.

Figure 4b shows the behavior of the analyzed designs when the exergy efficiency is evaluated with the environmental impact. As can be observed, to increase the efficiency it is necessary to increase the environmental impact as well.

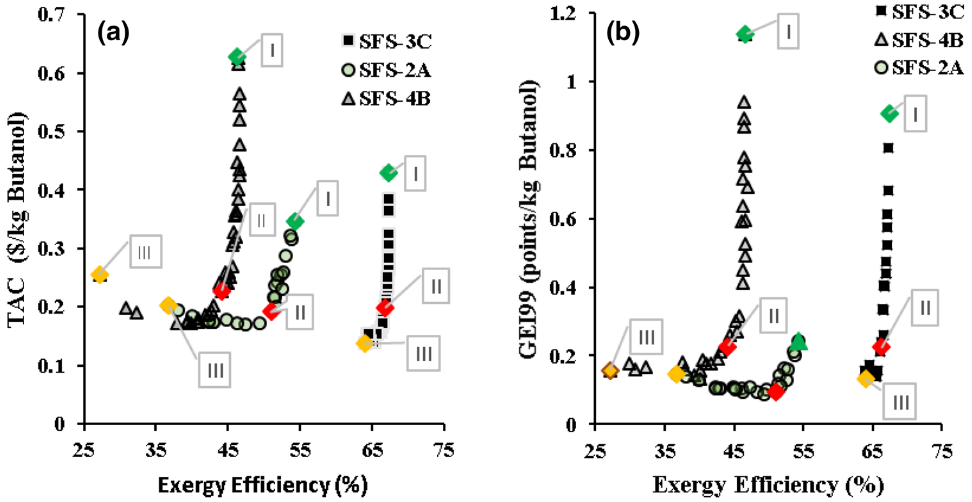

Fig. 4 Pareto fronts: **a** TAC with exergetic efficiency and **b** GEI99 with exergetic efficiency

In this case, the lowest environmental load was observed for the whole process which considers the purification stage by the process SFS-2A. This behavior is related with the previous selection of raw materials.

In Fig. 5, the best point of each scheme (point II) is highlighted. Performing a deeper analysis about the contribution regarding the TAC and the GEI99, note that for schema SFS-3C in Fig. 5a, low thermodynamic efficiencies are related with low cost values. Moreover, the main contribution to the TAC is due to the cost of the reactor, followed by the cost of raw material and finally the cost associated with the purification stage. This behavior is closely linked to the characteristics of the selected raw material (cost, sugar available and environmental impact). On the other hand, thermodynamic efficiency increases because of purification costs, and raw material costs and the reactor cost increases as well.

In the same way, the contribution to the GEI99 is shown in Fig. 5b, where the main contribution to the GEI99 is due to the raw material. One may notice that for high thermodynamic efficiencies the ecoindicator tends to increase significantly. This behavior is due to the use of raw material with great environmental impact which is also associated with a greater amount of available sugar.

For each analyzed scheme, Table 5 shows the most representative values related to economic and environmental indexes. Note the lowest value for raw material was obtained for the scheme SFS-2A with 0.0042 $\$/\mathrm{kg}_{\mathrm{butanol}}$ followed by scheme SFS-3C and SFS-4B, respectively. Regarding the environmental impact, the scheme SFS-4B exhibited the best value with 0.112 $\mathrm{points/kg}_{\mathrm{butanol}}$ followed by schemes SFS-3C and SFS-2A.

For the scheme SFS-4B in Fig. 5c, d, a similar trend is observed that is described for the scheme SFS-3C. However, for this scheme the low thermodynamic efficiencies are associated with the raw material cost, in other words, if the process uses more expensive raw materials, the thermodynamic efficiency increases as well. Note in this scheme the lowest TAC contribution is related with the raw material selection. On the other hand, the purification stage provides the main contribution. So, the manner in which this process route increases its thermodynamic efficiency, it also increases the purification cost. In the case of this scheme presented in Fig. 5d, the main contribution of the ecoindicator is largely due to the raw material. This scheme is not actually efficient in the purification stage, and in this manner, the reaction stage should provide better performance.

Figure 5e shows a similar behavior, and the low thermodynamic efficiencies are related to low raw material cost. In this manner, the main contribution to the TAC is attributed to the TAC in reaction stage. For high thermodynamic efficiencies again the three zones cost increase in a similar way. Figure 5f shows the contribution to the GEI99 of each analyzed area, being the less efficient stages both the purification stage and raw materials.

In a relative deeper analysis for the best point found (point II of scheme SFS-3C) in Fig. 6, it is possible to observe each category and the contribution for the total ecoindicator 99. Note that to carry out this environmental process, we considered the environmental loads of three sources: steam for heating, electricity for pumping and steel for building.

Thus, as Fig. 6 shows that due to using electricity and steam, the biggest impact is found in the fossil fuels category. On the other hand, the use of steel for building impacts directly ecotoxicity and use of minerals. To summarize the environmental impact in those three sources previously mentioned, Fig. 6 shows the environmental impact for each source.

Figure 7a, b shows the energetic performance of all analyzed schemes. In other words, both figures illustrate the performance of those whole processes which consider three different schemes as purification stages. Note the preferable behavior in the whole process is to consume energy as low as possible and increasing the exergy efficiency.

Under this expected behavior, Fig. 7 a shows the behavior of the energy consumed per kilogram of butanol and the exergy efficiency. With this in mind, the best results obtained concerning scheme SFS-3C which exhibited the lowest energy consumption are evident. However, one can notice the average behavior of all Pareto fronts is that as long as the energy consumption increases also increases the exergy efficiency. Considering the above mentioned, it is necessary to select a single design from the zone where both exergy and energy efficiencies reach a relative good value. Thus, in Fig. 7a was selected a point, which is highlighted in Pareto front. Concerning scheme SFS-3C, this selected point exhibited a thermodynamic efficiency of 66.80% and an energy consumption of 7.6 $\mathrm{MJ/kg}_{\mathrm{butanol}}$. On the other hand, the worst observed values were obtained by the scheme SFS-4B, with exergy efficiency of 44.13% and energy consumption of 17.78 $\mathrm{MJ/kg}_{\mathrm{butanol}}$. In the same way, in Fig. 7b it is possible to observe that the scheme SFS-3C generates a greater IES and the scheme SFS-4B generates less IES with values of 6.77 $\mathrm{MJ/kg}_{\mathrm{glucose}}$ and 5.32 $\mathrm{MJ/kg}_{\mathrm{glucose}}$, respectively.

Furthermore, Fig. 8 shows the variation of the process cost when the concentration of acetone, butanol and ethanol also vary in the feed stream of the purification process. In concordance with all results observed so far, the whole process with scheme SFS-3C shows the lowest TAC values, followed by scheme SFS-2A and SFS-4B. Moreover, note the better-feed stream has values like 1258.29, 1332.13, 1278.61, $\mathrm{kmol}_{\mathrm{ABE\text{-}ext}}$ for SFS-3C, SFS-2A and SFS-4B schemes, respectively.

Figure 9a, c shows the oscillation of the cost and sale price regarding the plant capacity. It can be clearly observed a tendency, the cost and sale price decrease when the plan

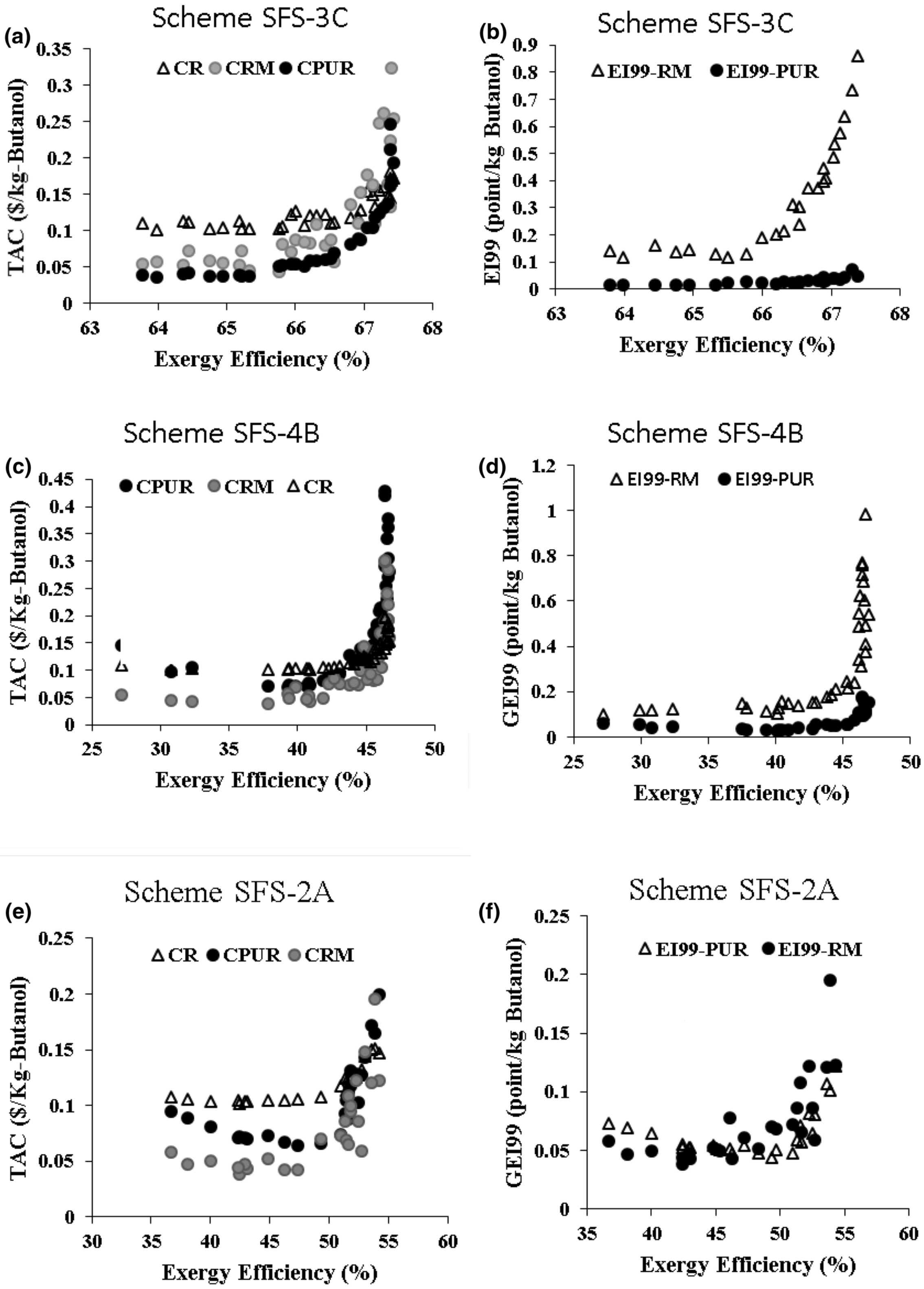

Fig. 5 Contribution of TAC, ecoindicator 99 and exergy efficiency for each of the analyzed scheme

Table 5 Summary of the main indexes for the raw material section for three representative designs on the Pareto front

Parameter	SFS-3C			SFS-4B			SFS-2A		
	I	II	III	I	II	III	I	II	III
Cost of raw material ($/kg$_{butanol}$)	0.057	0.135	0.213	0.058	0.077	0.300	0.042	0.073	0.123
Ecoindicator 99 (points/kg$_{butanol}$)	0.118	0.373	0.523	0.112	0.341	0.716	0.144	0.164	0.478

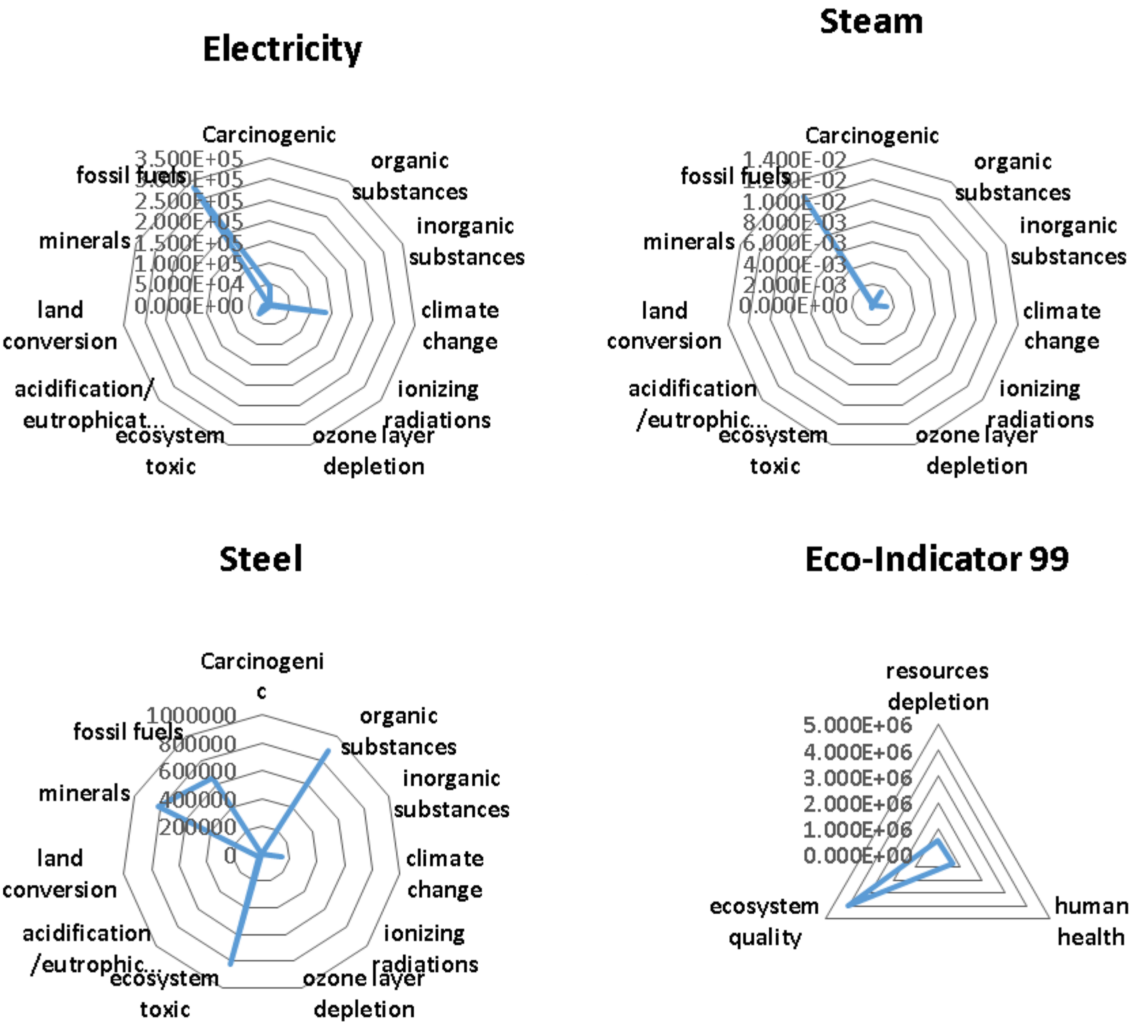

Fig. 6 Detailed contribution of the ecoindicator in its main sections and impact sources for the best point select

capacity increases. In this tendency, scheme SFS-3C shows the lowest cost values and sale price. In this manner, when the plant operates at low production capacity, there is a difference of almost 70% among some schemes. Specifically, a huge difference is observed among both SFS-3C and SFS-4B schemes. On the other hand, at high capacity production this difference diminishes significantly.

Furthermore, Fig. 9b shows the evaluation of the return of investment (ROI) regarding to the plant capacity. Notice that this scheme SFS-3C shows the best values overcoming both schemes SFS-2A and SFS-4B. Considering this economic behavior, it is clear that scheme SFS-3C always shows better economic benefits in comparison with the other studied scenarios.

Fig. 7 Energy indicators regarding exergy efficiency. **a** Exergy with NEB and **b** exergy efficiency with IES

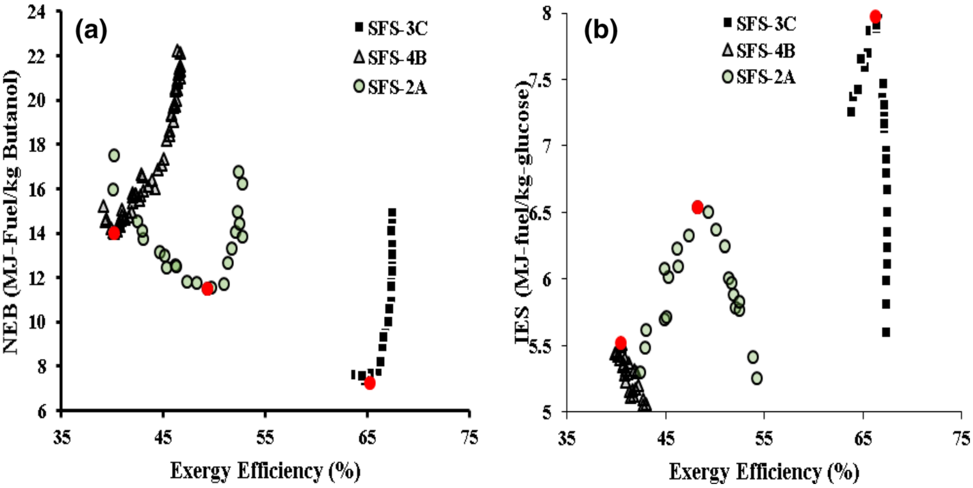

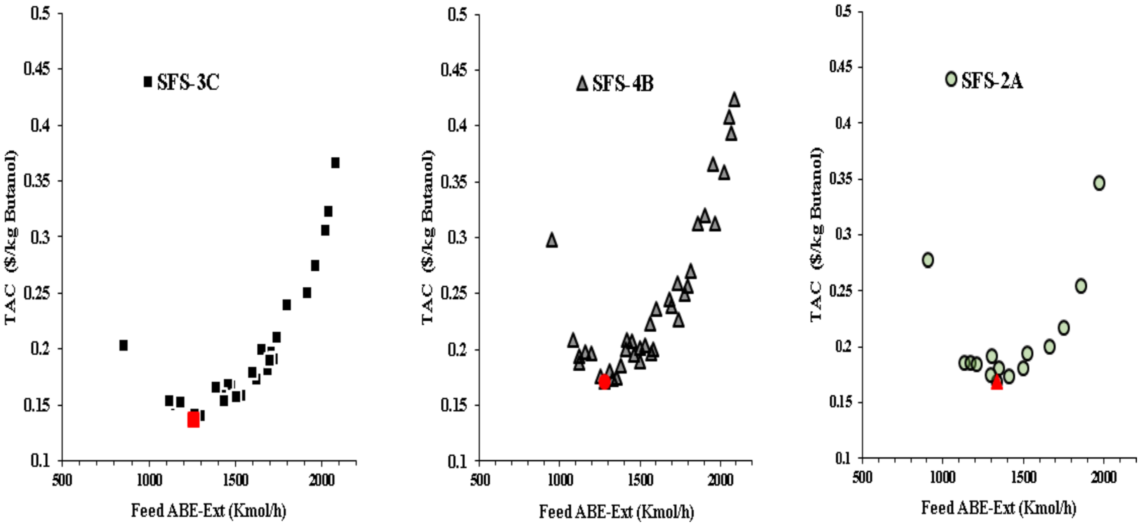

Fig. 8 Variation of cost respect to the molar flow of feed stream at the separation zone

As has been mentioned, increasing the production the economic scenario improves. In almost all economic scenarios scheme, SFS-3C showed the best economic indexes. However, we decided to consider additionally another economic index, the net present value (NPV) which allowed us to figure out if the investment accomplished its basic financial target: to maximize the investment.

The benefit of the exergy analysis goes beyond the application of the second thermodynamic law, which constitutes the base of the exergy methods. The second thermodynamic law might indicate the theoretical limits of efficiency in a reversible process. Figures 4 and 8 demonstrate how those limits vary on each process. Figure 10a presents the Pareto front generated when is evaluated the exergy efficiency with the NPV values. It is important to remember we tried to maximize the NPV value jointly with the energy efficiency. However, according to the behavior observed, both objective functions are in conflict, and one can observe the highest values of energy efficiency are found with low NPV values and vice versa. Thus, must be selected a single point from both objective functions reach its best value.

The reader can observe in Fig. 7b that again the scheme SFS-3C shows the best values for both objective functions since higher NPV and exergy efficiency values are observed. On the other hand, the process which includes scheme SFS-4B demonstrated again the worse NPV and exergy efficiency values.

As mentioned previously, the amount of sugar fed to the fermenter is mainly responsible for the final concentration of products in the outflow. Moreover, since it is not always the same raw material considered in the fermenter, different butanol flows are obtained throughout the year.

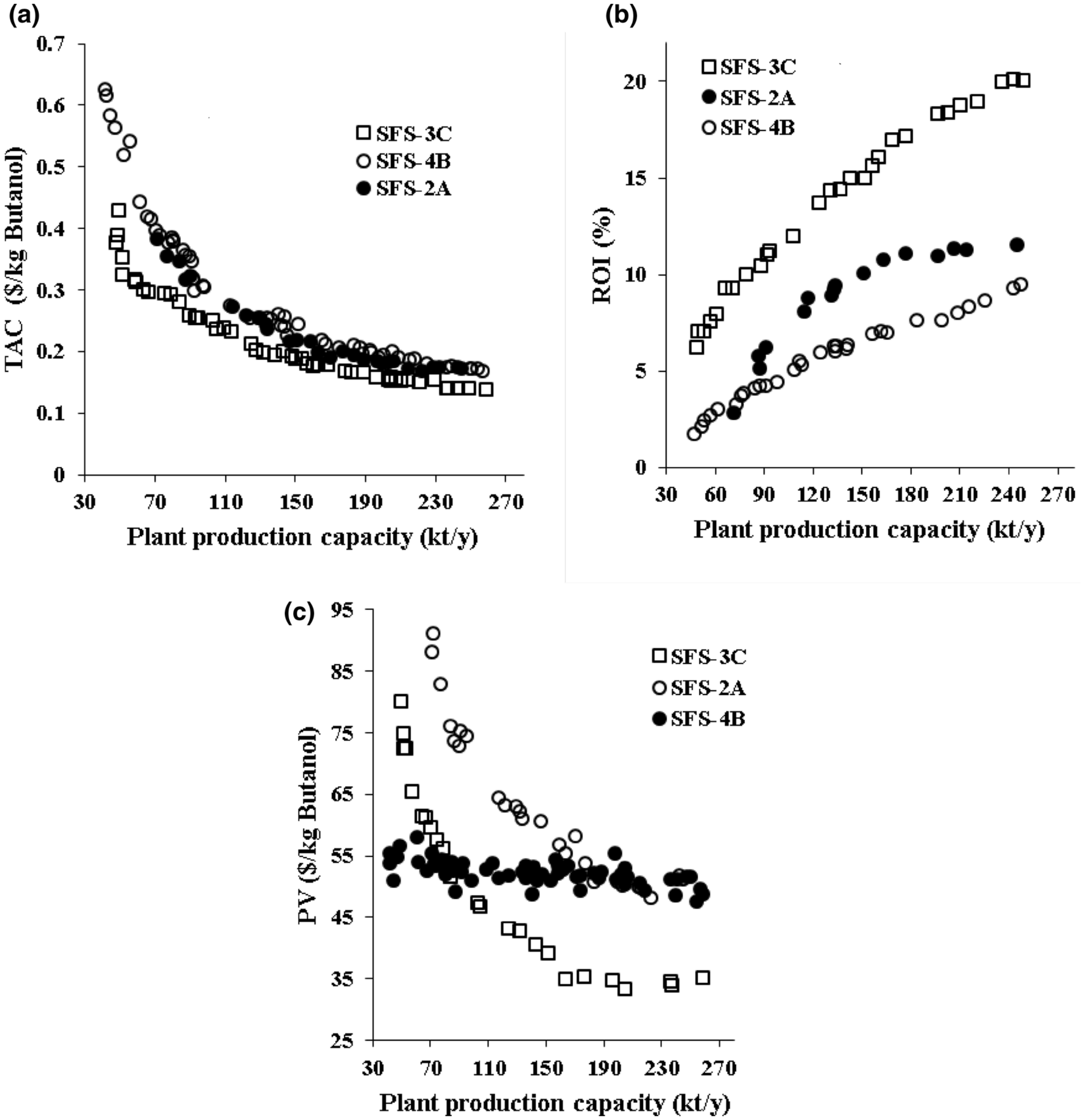

Fig. 9 **a** Evaluation of TAC with the plant capacity. **b** ROI with plant capacity and **c** sale price versus plant capacity

It is important to keep in mind that the value of the net present value depends on the following variables: initial investment, investments during the operation, net cash flows, discount rate and time of the project.

Figure 10b, c displays the behavior of the NPV with respect to the TAC and the GEI99. According to previous sections, the greatest economic benefit is obtained with higher NPV values which are obtained when the cost of the process decrease. It can be seen that the scheme SFS-3C has the highest values of NPV. The SFS-2A and SFS-4B schemes showed similar values; however, SFS-3C schemes exhibited a little improvement.

The variation of the environmental impact follows an even more marked trend than the cost, while the scheme SFS-2A showed the lowest environmental impacts, but low NPV. On the contrary, scheme SFS-3C displayed the highest NPV values but a lower environmental impact. It is important to mention that those values are not the smallest, however, are in the zone of the minimum values.

Clearly, the value of NPV can be taken as a distinctive economic criteria in order to select the best scheme. Regarding the use of energy, we can observe different behaviors from those previously analyzed.

Figure 11a shows the behavior of the economic objective function when is evaluated with the energy target. According to the Pareto front, the most energy generated the most NPV obtained. However, scheme SFS-3C presents the best values of NPV and higher energy generated as well. This scheme

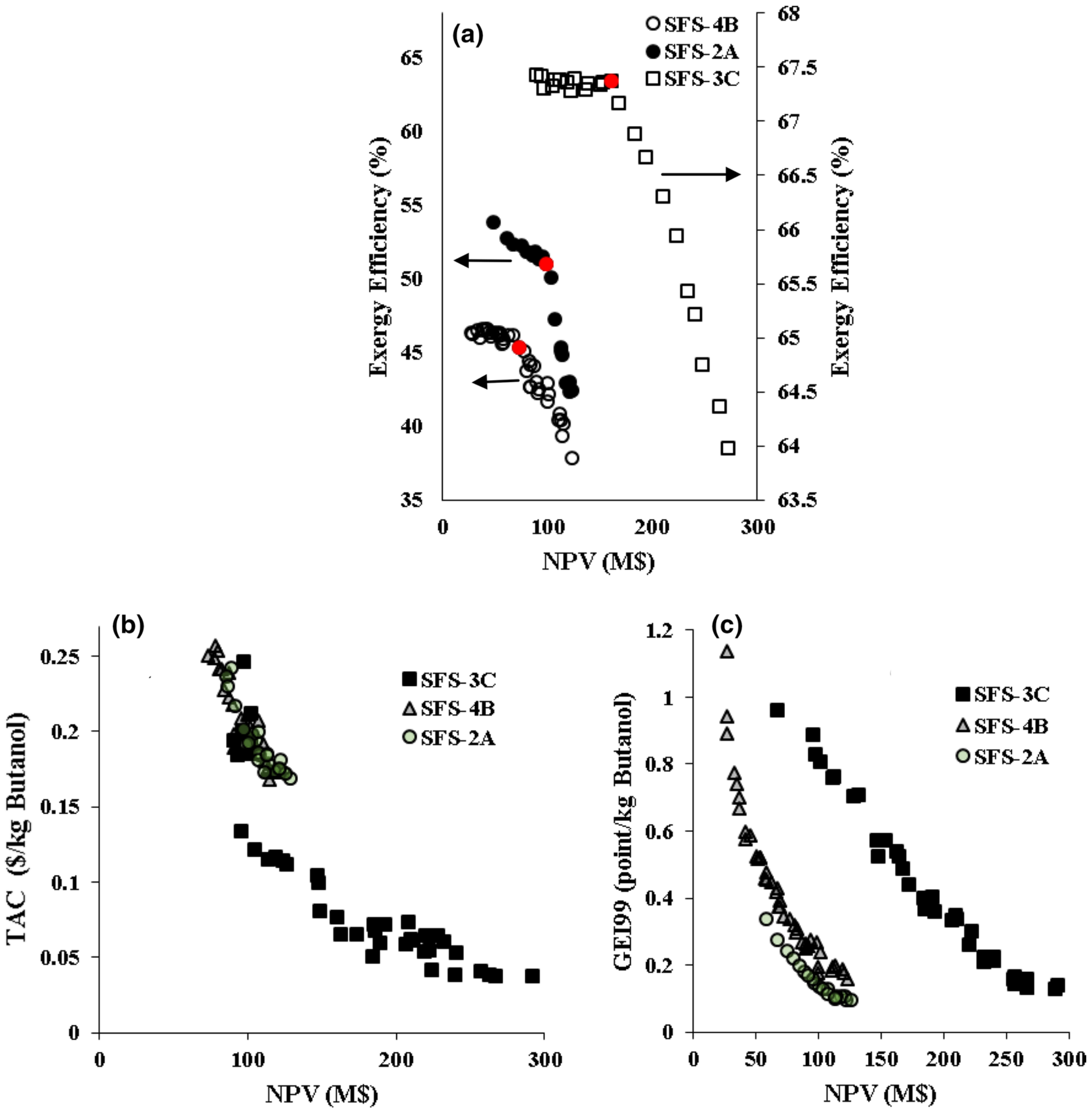

Fig. 10 Pareto front: **a** TAC evaluated with NPV, **b** ecoindicator 99 evaluated with NPV

covers a wide range of values, contrary to schemes SFS-2A and SFS-4B where NPV values are centered in a small range. However, all the three analyzed schemes showed very similar values.

A similar analysis is presented in Fig. 11b where the value of NPV is compared with the IES. The higher values of IES and NPV are for the SFS-3C scheme, which is the best performance scheme. On the other hand, the scheme with the lowest values of IES and NPV was scheme SFS-4B.

The trend is that the economic benefit measured through the NPV is in conflict with the energy values. It can be seen that scheme SFS-4B presents the highest values of energy requirements, contrary to scheme SFS-3C, which presents the lowest values.

On the other hand, Fig. 12 presents the optimal planning of raw material for scheme SFS-3C (Fig. 4, point II). Note a clear tendency to use corn grain and wheat as raw materials. This selection is completely due to the amount of sugar present in each raw material. Yet, the most sugar content the most expensive becomes the process, so it must be selected a correct combination of raw material with high sugar content and cheap raw materials. Therefore, the planning presented in Fig. 12 represents the best planning to equilibrate and reach the best values of the objective functions.

Moreover, Fig. 13 shows the correct selection of raw material for scheme SFS-2A. Note in this process the best values converges in sugar cane as main raw material. As well as SFS-3C scheme, this selection totally regards to raw

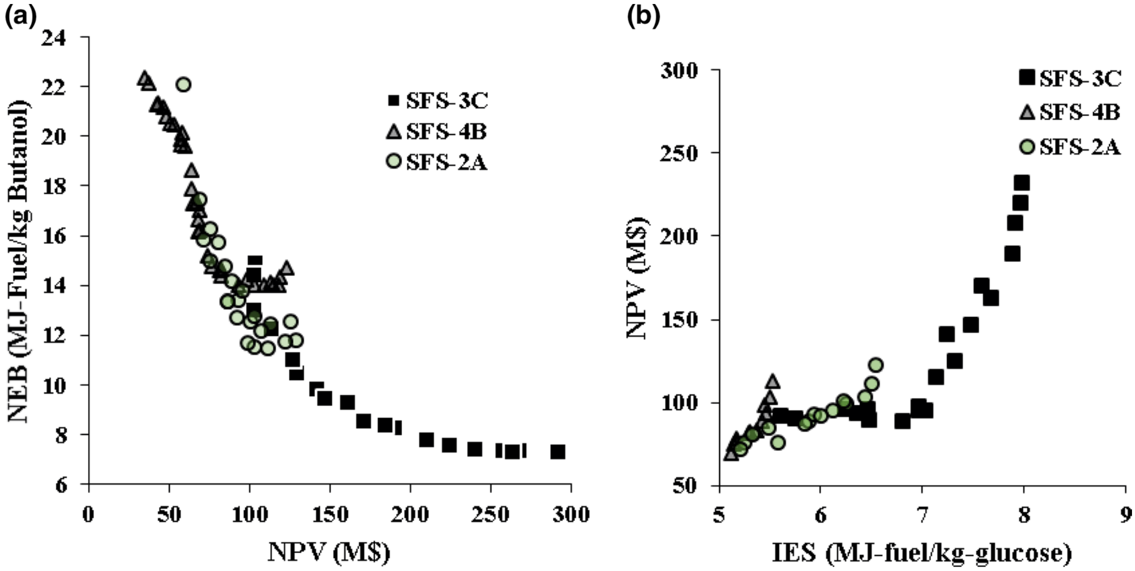

Fig. 11 Evaluation of NPV values with: **a** NEB, **b** IES

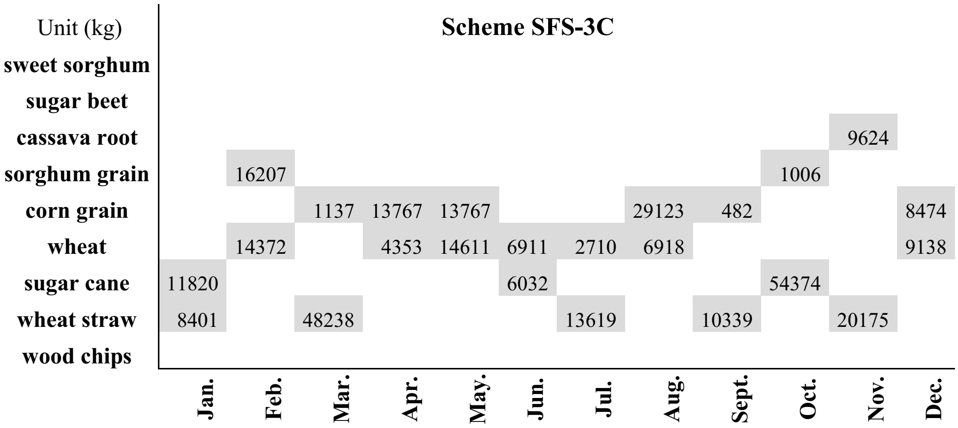

Fig. 12 Planning of raw material through the year for the best design in Pareto front of scheme SFS-3C

Scheme SFS-3C

Unit (kg)	Jan.	Feb.	Mar.	Apr.	May.	Jun.	Jul.	Aug.	Sept.	Oct.	Nov.	Dec.
sweet sorghum												
sugar beet												
cassava root											9624	
sorghum grain		16207								1006		
corn grain			1137	13767	13767			29123	482			8474
wheat		14372		4353	14611	6911	2710	6918				9138
sugar cane	11820					6032				54374		
wheat straw	8401		48238				13619		10339		20175	
wood chips												

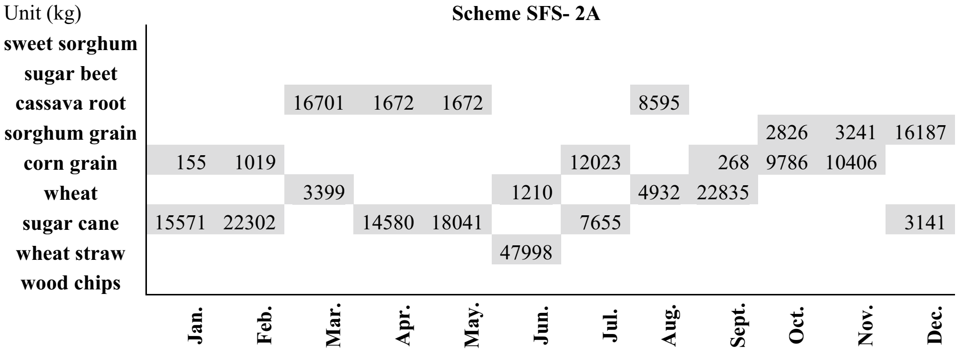

Fig. 13 Raw material planning throughout the year for the best selected point in scheme SFS-2A

Scheme SFS- 2A

Unit (kg)	Jan.	Feb.	Mar.	Apr.	May.	Jun.	Jul.	Aug.	Sept.	Oct.	Nov.	Dec.
sweet sorghum												
sugar beet												
cassava root			16701	1672	1672			8595				
sorghum grain										2826	3241	16187
corn grain	155	1019					12023		268	9786	10406	
wheat			3399			1210		4932	22835			
sugar cane	15571	22302		14580	18041		7655					3141
wheat straw						47998						
wood chips												

materials with high sugar content; however, this raw material is more expensive and the trend is to balance this cost with a cheaper raw material. As concern to the environmental impact, at the beginning of the year, as long as the year goes forward was selected raw materials with high environmental impacts according to the availability of raw material.

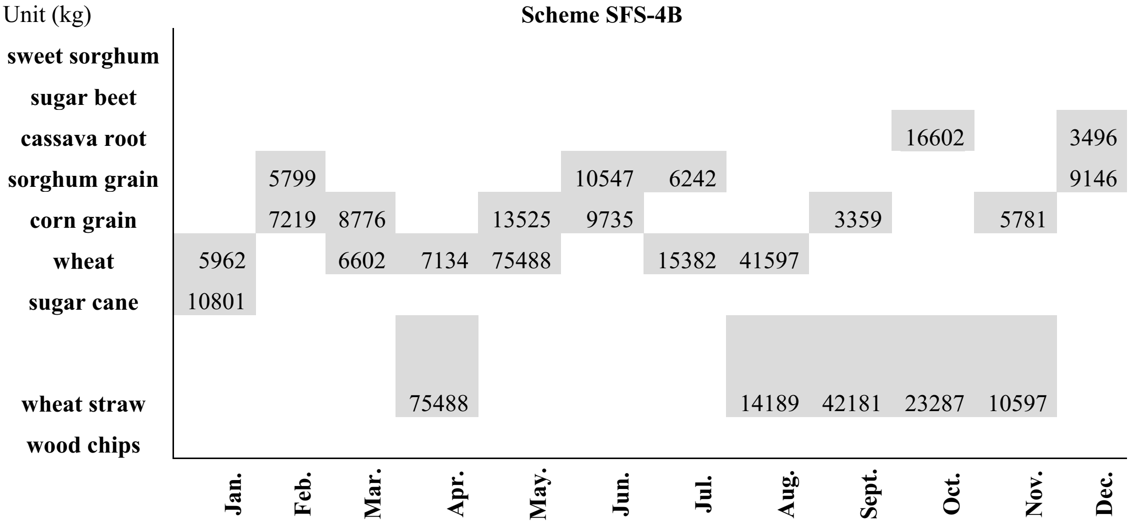

Unit (kg)	Jan.	Feb.	Mar.	Apr.	May.	Jun.	Jul.	Aug.	Sept.	Oct.	Nov.	Dec.
sweet sorghum												
sugar beet												
cassava root										16602		3496
sorghum grain		5799				10547	6242					9146
corn grain		7219	8776		13525	9735			3359		5781	
wheat	5962		6602	7134	75488		15382	41597				
sugar cane	10801											
wheat straw				75488				14189	42181	23287	10597	
wood chips												

Fig. 14 Planning of raw material through the year for the best design in Pareto front of scheme SFS-4B

Table 6 Summary of the main indexes of the integrated reactor for three representative points of the Pareto front

Parameter	SFS-3C			SFS-4B			SFS-2A		
	I	II	III	I	II	III	I	II	III
Productivity of butanol (g/L h)	0.7384	0.6703	0.3861	0.7279	0.7308	0.3417	0.7088	0.6548	0.4883
Yield of butanol (g/g)	0.309	0.332	0.338	0.314	0.327	0.341	0.321	0.316	0.346
Concentration of butanol in the fermentor (g/L)	6.8	5.2	3.0	6.7	5.6	2.7	6.3	5.5	3.9
Dilution rate (L^{-1})	0.0198	0.0175	0.0122	0.0103	0.0184	0.0192	0.0193	0.0199	0.0119
Extract (kg/kg$_{\text{butanol}}$)	50.05	65.3	69.91	50.12	66.4	67.95	52.75	58.5	68.45

Table 7 Summary of the main indexes for the preaching processes for three representative points of the Pareto front

Parameter	SFS-3C			SFS-4B			SFS-2A		
	I	II	III	I	II	III	I	II	III
Destilation TAC (\$/kg$_{\text{butanol}}$)	0.0368	0.0808	0.2468	0.070	0.116	0.428	0.064	0.0738	0.199
Cost of installation (\$/kg$_{\text{butanol}}$)	0.0013	0.0019	0.0067	0.002	0.003	0.013	0.002	0.0026	0.005
Cost of utilities (\$/kg$_{\text{butanol}}$)	0.0355	0.0789	0.2401	0.067	0.112	0.415	0.062	0.0711	0.195
Ecoindicator of distillation section (points/kg$_{\text{butanol}}$)	0.0133	0.0296	0.0903	0.029	0.048	0.176	0.044	0.0476	0.122
Internal rate of return (% year^{-1})	18.09	11.49	7.05	7.62	5.97	1.82	12.42	9.60	7.85
Production capacity (kton/año)	2586	1514	495	2542	1738	417	2223	1699	839
Sale price (\$/kg$_{\text{butanol}}$	35.22	39.17	80.09	47.62	49.42	55.41	52.08	58.23	76.11

Table 8 Summary of results of objective functions of the sequences for three representative points of the Pareto front

Parameter	SFS-3C			SFS-4B			SFS-2A		
	I	II	III	I	II	III	I	II	III
TAC ($\$/kg_{butanol}$)	0.138	0.198	0.429	0.172	0.227	0.626	0.169	0.192	0.347
GEI99 ($\$/kg_{butanol}$)	0.132	0.403	0.613	0.142	0.388	0.892	0.188	0.095	0.244
NEB ($MJ/kg_{butanol}$)	7.62	11.14	14.9	14.5	17.78	22.2	11.80	11.70	16.30
IES ($MJ/kg_{glucose}$)	7.37	6.77	5.60	5.32	4.49	3.16	6.33	6.25	5.25
NPV (M$)	266.4	148.7	107.8	211.4	161.8	51.1	251.3	192.4	146.3
Exergy efficiency (–)	64.0	66.8	67.4	39.3	44.1	46.4	64.0	47.4	54.3

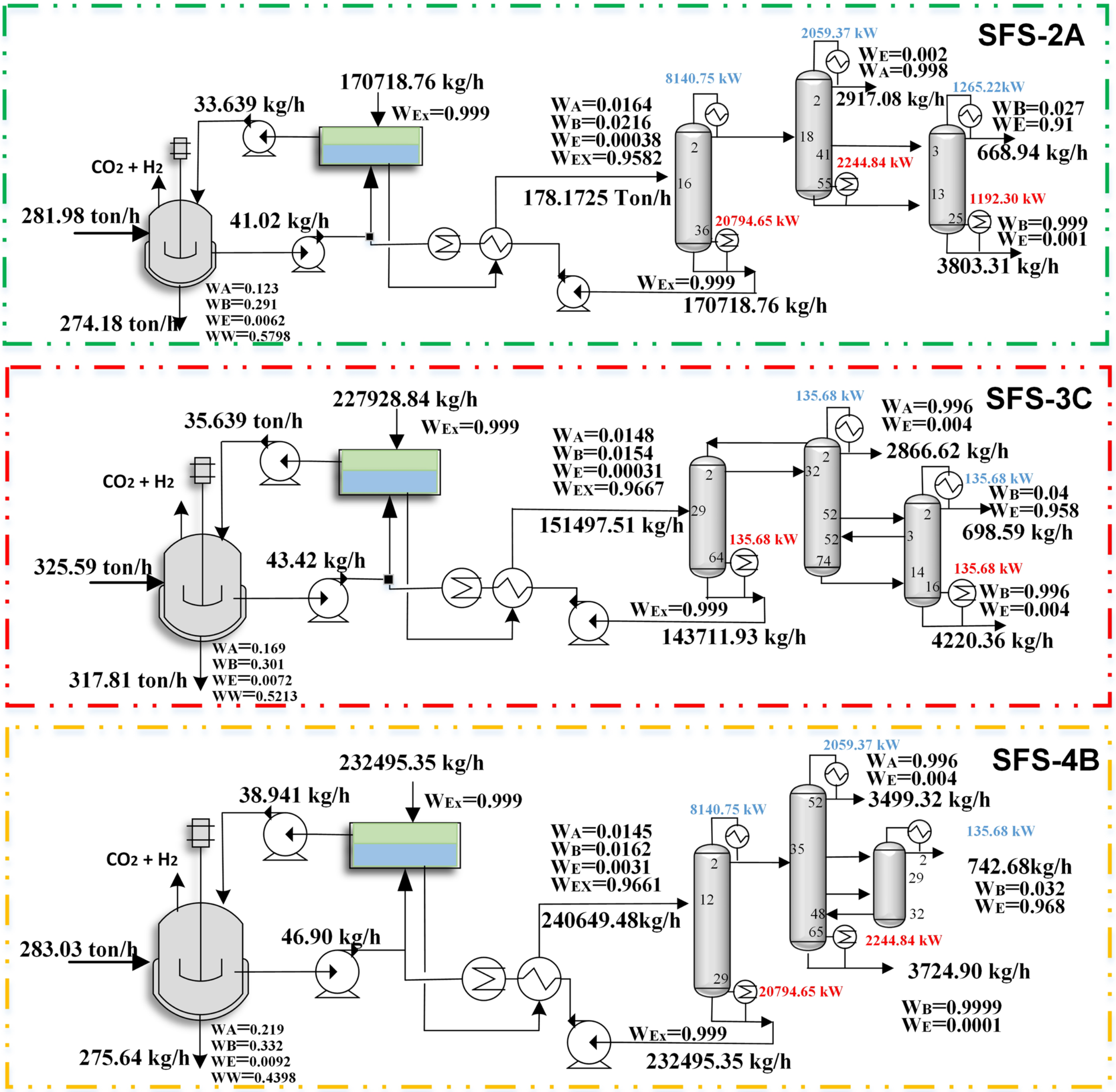

Fig. 15 Energy and mass balance of the whole process considering a different downstream process

Regarding scheme SFS-4B, Fig. 14 shows the planning of raw material for this scheme. This process prefers to use preferably wheat, wheat straw and corn grains. Those schemes selected raw material with high environmental impact. Such raw material selection is completely related with the sugar content, which consequently improves the performance at fermenter.

Table 6 illustrates the main parameters of the integrated reactor for each selected point in the Pareto front. The scheme SFS-3C has good performance with butanol concentration near 6.8 g/L and productivities of 0.738 g/L h. In the same way, Table 7 shows the main indexes considering only the purification/separation stage. In this scenario, the scheme SFS-3C overcomes the other designs with almost 50%. Because of this economic view, it was possible to obtain NPV values near to 19.09%.

On the other hand, Table 8 summarizes the three objective functions for each point selected in Pareto front which considers the whole process fermentation and purification. In this scenario, the scheme SFS-3C resulted as the best option with cost values of 0.138 $\$/\mathrm{kg}_{\mathrm{butanol,}}$ and an ecoindicator of 0.132 $\mathrm{points/kg}_{\mathrm{butanol}}$. Actually, this environmental impact is not the lowest; however, it generates the lowest energetic requirements near to 7.62 $\mathrm{MJ/kg}_{\mathrm{butanol}}$ and 7.37 $\mathrm{MJ/kg}_{\mathrm{butanol}}$ of generated energy. Finally, Fig. 15 presents the updated flow sheet of the best points of the best sequence analyzed, including the mass balance, energy requirements and design parameters. It should be pointed out that for each schema design, was a multi-objective optimization which obtained these best designs.

Conclusions

To determine the most feasible condition to produce butanol it must include rigorous simulations and even better a multi-objective optimization to evaluate several objective functions. This optimization will show the different areas, which promote any improvement in the process.

In general terms, the whole process which considers the separation stage by means of the scheme SFS-3C shows the best indexes with 0.138$\$/\mathrm{kg}_{\mathrm{butanol}}$, 0.132 $\mathrm{points/kg}_{\mathrm{butanol}}$, 66.8, 266.4 M$ and 2586 ton/year of TAC, GEI99, exergy efficiency, NPV and annual production, respectively. Moreover, the scheme SFS-3C exhibited the lowest energy requirements per kg of produced butanol with 5.7 $\mathrm{MJ/kg}_{\mathrm{butanol}}$ which is only 16% of the energy contained in 1 kg. of butanol. This reduction is a meaning improvement in comparison with the other scheme analyzed in this work and with other reported in the literature. For example, the results reported by Qureshi et al. (2005) with a process of adsorption–distillation presented an energy consumption of 8.2 $\mathrm{MJ/kg}_{\mathrm{butanol}}$. Moreover, if acetone and ethanol are also produced as by-products is considered, this profitability could increase. Regarding raw material selection, the most selected biomass was corn grain, wheat and wheat straw. Those raw materials were also selected in the scheme SFS-3C.

The multi-objective optimization carried out which includes the concepts of energy, exergy, cost and environmental impact have an important role to play in the evaluation and increase of the use of sustainable energy and technologies. The inclusion of energy and exergy in the design of the processes could be useful for identifying and improving processes.

Acknowledgements The financial support provided by the Universidad de Guanajuato and CONACyT (México) is gratefully acknowledged.

References

Akinci B, Kassebaum PG, Fitch JV, Thompson RW (2008) The role of bio-fuels in satisfying US transportation fuel demands. Energy Policy 36:3485–3491. https://doi.org/10.1016/j.enpol.2008.05.021

Andrié P, Meyer AS, Jensen PA, Dam-Johansen K (2010) Reactor design for minimizing product inhibition during enzymatic lignocellulose hydrolysis. II. Quantification of inhibition and suitability of membrane reactors. Biotechnol Adv 28:407–425

Azapagic A, Clift R (1999) The application of life cycle assessment to process optimisation. Comput Chem Eng 23:1509–1526

Barton WE, Daugulis A (1992) Evaluation of solvents for extractive butanol fermentation with *Clostridium acetobutylicum* and the use of poly(propylene glycol) 1200. Appl Microbiol Biotechnol 36:632–639. https://doi.org/10.1007/BF00183241

Bechara R, Gomez A, Saint-Antonin V et al (2016) Methodology for the design and comparison of optimal production configurations of first and first and second generation ethanol with power. Appl Energy 184:247–265. https://doi.org/10.1016/j.apenergy.2016.09.100

Bhattacharya SS, Garlapati VK, Banerjee R (2011) Optimization of laccase production using response surface methodology coupled with differential evolution. New Biotechnol 28:31–39. https://doi.org/10.1016/j.nbt.2010.06.001

Bonilla-Petriciolet A, Rangaiah GP, Segovia-Hernández JG (2010) Evaluation of stochastic global optimization methods for modeling vapor–liquid equilibrium data. Fluid Phase Equilib 287:111–125. https://doi.org/10.1016/j.fluid.2009.09.021

Cooksley CM, Zhang Y, Wang H et al (2012) Targeted mutagenesis of the *Clostridium acetobutylicum* acetone–butanol–ethanol fermentation pathway. Metab Eng 14:630–641. https://doi.org/10.1016/j.ymben.2012.09.001

Díaz VHG, Tost GO (2016a) Butanol production from lignocellulose by simultaneous fermentation, saccharification, and pervaporation or vacuum evaporation. Bioresour Technol 218:174–182. https://doi.org/10.1016/j.biortech.2016.06.091

Díaz VHG, Tost GO (2016b) Ethanol and isobutanol dehydration by heat-integrated distillation. Chem Eng Process 108:117–124

Edgerton RH (1992) Available Energy and Environmental Economics. D.C. Heath, Toronto

Errico M, Sanchez-Ramirez E, Quiroz-Ramìrez JJ et al (2016) Synthesis and design of new hybrid configurations for biobutanol purification. Comput Chem Eng 84:482–492. https://doi.org/10.1016/j.compchemeng.2015.10.009

Gapes JR (2000) The economics of acetone-butanol fermentation: theoretical and market considerations. J Mol Microbiol Biotechnol 2:27–32

Gassner M, Marechal F (2013) Increasing efficiency of fuel ethanol production from lignocellulosic biomass by process integration. Energy Fuels 27:2017–2115

Gebreslassie BH, Guillén-Gosálbez G, Jiménez L, Boer D (2009) Design of environmentally conscious absorption cooling systems via multi-objective optimization and life cycle assessment. Appl Energy 86:1712–1722. https://doi.org/10.1016/j.apenergy.2008.11.019

Goedkoop M, Spriensma R (2000) The Eco-indicator 99 A damage oriented method for Life Cycle Impact Assessment Methodology Annex

Groot WJ, Soedjak HS, Donck PB et al (1990) Butanol recovery from fermentations by liquid–liquid extraction and membrane solvent extraction. Bioprocess Eng 5:203–216

Groot WJ, Van Der LansRGJM, Luyben KCAM (1992) Technologies for butanol recovery integrated with fermentations. Process Biochem 27:61–75

Guthrie KM (1969) Capital cost estimating, Chemical Engineering, March 24, p 114

Jang YS, Malaviya A, Cho C et al (2012) Butanol production from renewable biomass by clostridia. Bioresour Technol 123:653–663

Kadam KL, Rydholm EC, McMillan JD (2004) Development and validation of a kinetic model for enzymatic saccharification of lignocellulosic biomass. Biotechnol Prog 20:698–705. https://doi.org/10.1021/bp034316x

Kheawhom S (2010) Efficient constraint handling scheme for differential evolutionary algorithm in solving chemical engineering optimization problem. J Ind Eng Chem 16:620–628. https://doi.org/10.1016/j.jiec.2010.03.004

Kiss AA, Lange JP, Schuur B et al (2016) Separation technology-making a difference in biorefineries. Biomass Bioenerg 95:296–309. https://doi.org/10.1016/j.biombioe.2016.05.021

Kumar S, Datta D, Babu BV (2011) Estimation of equilibrium parameters using differential evolution in reactive extraction of propionic acid by tri-*N*-butyl phosphate. Chem Eng Process Process Intensif 50:614–622. https://doi.org/10.1016/j.cep.2011.03.004

Lenz TG, Morelra AR (1980) Economic evaluation of the acetone–butanol fermantation. Ind Eng Chem Prod Res Dev 19(4):478–483

López-Maldonado LA, Ponce-Ortega JM, Segovia-Hernández JG (2011) Multiobjective synthesis of heat exchanger networks minimizing the total annual cost and the environmental impact. Appl Therm Eng 31:1099–1113. https://doi.org/10.1016/j.applthermaleng.2010.12.005

Luyben WL, Chien IL (2011) Design and control of distillation systems for separating azeotropes. Wiley, New York

Maddox IS (1989) The acetone–butanol–ethanol fermentation: recent progress in technology. Biotechnol Genet Eng Rev 7:189–220. https://doi.org/10.1080/02648725.1989.10647859

Mariano AP, Qureshi N, Maciel Filho R, Ezeji TC (2012) Assessment of in situ butanol recovery by vacuum during acetone butanol ethanol (ABE) fermentation. J Chem Technol Biotechnol 87:334–340. https://doi.org/10.1002/jctb.2717

Miranda-Galindo EY, Segovia-Hernández JG, Hernández S, Bonilla-Petriciolet A (2014) Multiobjective optimization of a hydrodesulfurization process of diesel using distillation with side reactor. Ind Eng Chem Res 53:16425–16435. https://doi.org/10.1021/ie501940v

Niemistö J, Saavalainen P, Isomäki R, Kolli T, Huuhtanen M, Keiski RL (2013) Biobutanol production from biomass. In: Gupta VK, Tuohy MG (eds) Biofuel technologies: recent developments. Springer, New York, pp 443–470

Oudshoorn A, van der Wielen LAM, Straathof AJJ (2009) Assessment of options for selective 1-butanol recovery from aqueous solution. Ind Eng Chem Res 48:7325–7336. https://doi.org/10.1021/ie900537w

Parekh M, Blaschek HP (1999) Butanol production by hypersolvent-producing mutant *Clostridium beijerinckii* BA101 in corn steep water medium containing maltodextrin. Biotechnol Lett 21:45–48. https://doi.org/10.1023/A:1005406120874

Quiroz-Ramírez JJ, Sánchez-Ramírez E, Hernández S et al (2017) Multiobjective stochastic optimization approach applied to a hybrid process production-separation in the production of biobutanol. Ind Eng Chem Res 56:1823–1833. https://doi.org/10.1021/acs.iecr.6b04230

Qureshi N, Blaschek HP (2000) Economics of butanol fermentation using hyper-butanol producing *Clostridium beijerinckii* BA101. Food Bioprod Process 78:139–144. https://doi.org/10.1205/096030800532888

Qureshi N, Blaschek HP (2001) ABE production from corn: a recent economic evaluation. J Ind Microbiol Biotechnol 27:292–297. https://doi.org/10.1038/sj/jim/7000123

Qureshi N, Hughes S, Maddox IS, Cotta MA (2005) Energy-efficient recovery of butanol from model solutions and fermentation broth by adsorption. Bioprocess Biosyst Eng 27:215–222. https://doi.org/10.1007/s00449-005-0402-8

Qureshi N, Singh V, Liu S et al (2014) Process integration for simultaneous saccharification, fermentation, and recovery (SSFR): production of butanol from corn stover using *Clostridium beijerinckii* P260. Bioresour Technol 154:222–228. https://doi.org/10.1016/j.biortech.2013.11.080

Ranjan A, Moholkar VS (2009) Biobutanol: a Viable Gasoline Substitute through ABE Fermentation. Proc Int Conf Energy Environ 51:497–503

Rosen MA, Dincer I, Kanoglu M (2008) Role of exergy in increasing efficiency and sustainability and reducing environmental impact. Energy Policy 36:128–137. https://doi.org/10.1016/j.enpol.2007.09.006

Santibañez-Aguilar JE, González-Campos JB, Ponce-Ortega JM et al (2014) Optimal planning and site selection for distributed multiproduct biorefineries involving economic, environmental and social objectives. J Clean Prod 65:270–294. https://doi.org/10.1016/j.jclepro.2013.08.004

Seader JD, Ernest JH, Roper DK (2011) Separation process principles-chemical and biochemical operations. Chemical and Biochemical Operations. Wiley, Hoboken, NJ

Sharma S, Rangaiah GP (2010) Separation process principles-chemical and biochemical operations, pp 978–981

Sharma S, Rangaiah GP (2013) An improved multi-objective differential evolution with a termination criterion for optimizing chemical processes. Comput Chem Eng 56:155–173. https://doi.org/10.1016/j.compchemeng.2013.05.004

Shinto H, Tashiro Y, Yamashita M et al (2007) Kinetic modeling and sensitivity analysis of acetone–butanol–ethanol production. J Biotechnol 131:45–56. https://doi.org/10.1016/j.jbiotec.2007.05.005

Shinto H, Tashiro Y, Kobayashi G et al (2008) Kinetic study of substrate dependency for higher butanol production in acetone–butanol–ethanol fermentation. Process Biochem 43:1452–1461

Srinivas M, Rangaiah GP (2007) Differential Evolution with Tabu List for solving nonlinear and mixed-integer nonlinear programming problems. Ind Eng Chem Res 46:7126–7135

Szargut J, Morris DR, Steward FR (1988) Exergy analysis of thermal, chemical, and metallurgical processes. Springer

Tashiro Y, Sonomoto K (2010) Advances in butanol production by clostridia. Curr Res Technol Educ Top Appl Microbiol Microbial Biotechnol 2:1383–1394

Tijmensen MJA, Faaij APC, Hamelinck CN, Van Hardeveld MRM (2002) Exploration of the possibilities for production of Fischer Tropsch liquids and power via biomass gasification. Biomass Bioenerg 23:129–152. https://doi.org/10.1016/S0961-9534(02)00037-5

Turton R, Whiting B, Bailie CR et al (2012) Analysis, synthesis, and design of chemical processes, 4th ed

Ulrich GD (1984) A guide to chemical engineering process design and economics. Wiley, New York, p 295

Vakili R, Setoodeh P, Pourazadi E et al (2011) Utilizing differential evolution (DE) technique to optimize operating conditions of an integrated thermally coupled direct DME synthesis reactor. Chem Eng J 168:321–332. https://doi.org/10.1016/j.cej.2011.01.032

Van der Merwe AB, Cheng H, Görgens JF, Knoetze JH (2013) Comparison of energy efficiency and economics of process designs for biobutanol production from sugarcane molasses. Fuel 105:451–458. https://doi.org/10.1016/j.fuel.2012.06.058

Vázquez-Castillo JA, Segovia-Hernández JG, Ponce-Ortega JM (2015) Multiobjective optimization approach for integrating design and control in multicomponent distillation sequences. Ind Eng Chem Res 54:12320–12330. https://doi.org/10.1021/acs.iecr.5b01611

Wooley RJ, Putsche V (1996) Development of an ASPEN PLUS physical property database for biofuels components

Wu M, Wang M, Liu J, Huo H (2008) Assessment of potential life-cycle energy and greenhouse gas emission effects from using corn-based butanol as a transportation fuel. Biotechnol Prog 24(6):1204–1214

Xue C, Zhao X-Q, Liu C-G et al (2013) Prospective and development of butanol as an advanced biofuel. Biotechnol Adv 31:1575–1584. https://doi.org/10.1016/j.biotechadv.2013.08.004

Xue C, Zhao J, Chen L (2014) Integrated butanol recovery for an advanced biofuel: current state and prospects. Appl Microbiol Biotechnol 98:3463–3474. https://doi.org/10.1007/s00253-014-5561-6

Yerramsetty KM, Murty CVS (2008) Synthesis of cost-optimal heat exchanger networks using differential evolution. Comput Chem Eng 32:1861–1876. https://doi.org/10.1016/j.compchemeng.2007.10.005